Received: 11 June 2020 | Revised: 4 November 2020 | Accepted: 23 November 2020

DOI: 10.1049/cds2.12040

IET Circuits, Devices & Systems

The Institution of Engineering and Technology WILEY

ORIGINAL RESEARCH PAPER

Time-interleaving design of error-feedback sigma-delta modulators with infinite impulse response noise transfer function

Francisco Colodro | **Juana Maria Martinez-Heredia** | **Jose L. Mora** | **Antonio Torralba**

Electronic Engineering Department, Universidad de Sevilla, Escuela Superior de Ingenieros, Sevilla, Spain

Correspondence

Jose L. Mora, Electronic Engineering Department, Universidad de Sevilla, Escuela Superior de Ingenieros, Camino de los Descubrimientos s/n, 41092, Sevilla, Spain.
Email: jolumo@us.es

Funding information

Spanish Ministry of Science, Innovation and Universities, Grant/Award Number: RTI2018-099189-B-C21

Abstract

Transceivers built to modern communication standards tend to be as digital as possible, including the radio-frequency stages. This forces the digital-to-analogue converters (DACs) in the transmitter section to have a large bandwidth. DACs based on sigma-delta (SD) modulation represent a good choice in modern digital technologies as they have a simple analogue circuitry with limited accuracy requirements. Error-feedback (EF) architectures are widely used in the realisation of SD modulators. In many applications, DAC output has a small number of bits. In that case, the noise transfer function (NTF) must be of high order (to achieve a high dynamic range) and of the infinite impulse response (IIR) type (for the sake of stability). Concerning its implementation, one of the main challenges comes from the speed limitation of the technology. In this sense, time-interleaving (TI) allows the designer a trade-off between complexity and speed. Transforming the EF architecture into its TI counterpart is not straightforward for IIR NTFs. A procedure for this transformation is proposed, and a case study is described for a third-order modulator. A method of coefficient rounding is also proposed to simplify the digital implementation of the modulator while avoiding mismatches between the parallel paths of the TI modulator.

1 | INTRODUCTION

Sigma-delta modulators (SDMs) are increasingly receiving attention in the implementation of modern communication standards in the design of both transmitters and receivers. Wideband software-defined transmitters require the digital-to-analogue converter (DAC) to be rated at a very high frequency [1–4]. When an SDM-based DAC is used, speed constraints of the hardware impose moderate values of the oversampling ratio (OSR) [5]. As a result, the required dynamic range (DR) can only be achieved using high-order SDMs. When the noise transfer function (NTF) is a finite impulse response (FIR) filter, high-order modulators can be stable as long as the bit number of the quantiser is equal to or larger than $L + 1$, where L is the order of the modulator [6]. On the other hand, single-bit DACs present the nice feature that they can directly drive an energy-efficient switching-mode power amplifier or the laser in a radio-over-fibre architecture [1].

Moreover, the simplicity and relaxed requirements of the single-bit DAC (where mismatch is not a concern, so complex linearisation techniques, such as dynamic element matching [5], are not necessary) facilitate the realisation of its analogue part at very high frequencies. Unfortunately, single-bit high-order SDMs are prone to instability, so for the sake of stability, the NTF must be of the infinite impulse response (IIR) type; that is,

$$NTF(z) = \left(1 - z^{-1}\right)^L \Big/ D(Z) \tag{1}$$

where L is the order of the modulator and $D(z)$ is an L-order polynomial in z [5]. Consequently, in an error-feedback (EF) realisation (Figure 1), the loop filter is also of the IIR type:

$$H(z) = NTF(z) - 1\left[\left(1 - z^{-1}\right)^L - D(Z)\right] \Big/ D(z) \tag{2}$$

In order to gain speed, different techniques for the decomposition of arbitrary-order IIR transfer functions have been proposed [7–15]. Time-interleaving (TI) has been used to

overcome or alleviate speed constraints in the implementation of SDMs [9–12]. The modulator of Figure 1, clocked at the sampling frequency f_s, is decomposed in N parallel paths clocked at the low rate f_s/N, by means of the filter bank $\overline{H}(z)$ shown in Figure 2 [10]. The filter bank $\overline{H}(z)$ can be obtained from $H(z)$ by means of type I polyphase decomposition (PD) [13]:

$$H(z) = \sum_{i=0}^{N-1} z^{-i} H_i(z^N) \tag{3}$$

where $H_i(z)$ are the components of $H(z)$. This decomposition is straightforward for a FIR transfer function or first-order simple sections of the type $1/(1-a\,z^{-1})$, but it is a complex task for a general IIR transfer function like that in (2). Once the functions $H_i(z)$ are known, the filter bank can be calculated by [10, 13]:

$$\bar{H}(z) = \begin{bmatrix} H_0(z) & H_1(z) & H_2(z) & \dots & H_{N-1}(z) \\ z^{-1}H_{N-1}(z) & H_0(z) & H_1(z) & \dots & H_{N-2}(z) \\ z^{-1}H_{N-2}(z) & z^{-1}H_{N-1}(z) & H_0(z) & \dots & H_{N-3}(z) \\ \vdots & \vdots & \vdots & \ddots & \vdots \\ z^{-1}H_1(z) & z^{-1}H_2(z) & z^{-1}H_3(z) & \dots & H_0(z) \end{bmatrix} \tag{4}$$

Due to the inherent advantages of DACs based on a single-bit SDM, the performance improvement of high-order modulators, and the capability of TI architectures to increase the effective operation rate, the design of an SDM that combines these features is addressed by the authors. Although some examples can be found in the design of cascaded high-order SDMs, this is the first time, to the best knowledge of the authors, that a digital single-bit high-order EF structure with an IIR NTF has been designed. For practical reasons, in the real-world implementation of this architecture, the floating-point coefficients of filter $H(z)$ in Figure 1 must be rounded. The rounding must be carefully carried out in order to maintain the NTF zeros in their ideal position ($z = 1$). Failure to do so could lead to decreases in performance. For this purpose, a novel rounding procedure is also proposed herein. In the following section, the polyphase decomposition is reviewed. Afterwards, a third-order EF structure is developed, coefficient rounding is completed, and the resulting architecture is evaluated by simulation results.

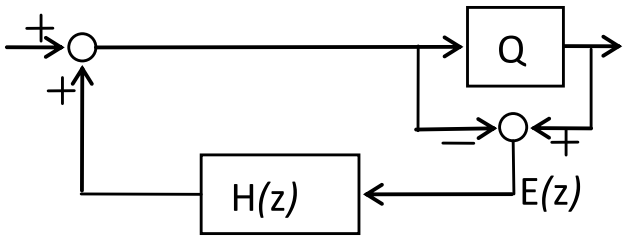

FIGURE 1 Error-feedback sigma-delta modulator architecture

2 | POLYPHASE DECOMPOSITION

In order to carry out PD when the transfer function is an IIR filter, $H(z)$ should be reformulated as [14,15]

$$H(z) = Q(z)/P(z^N) \tag{5}$$

where $Q(z)$ and $P(z)$ are polynomials in z. In this way, the PD of $H(z)$ results in the components

$$H_i(z) = Q_i(z)/P(z) \tag{6}$$

where $Q_i(z)$ ($i = 0,1,\ldots, N-1$) are the components of the (type I) PD of $Q(z)$ [13],

$$Q_i(z) = \sum_{k=0}^{+\infty} q_{kN+i}\, z^{-k} \tag{7}$$

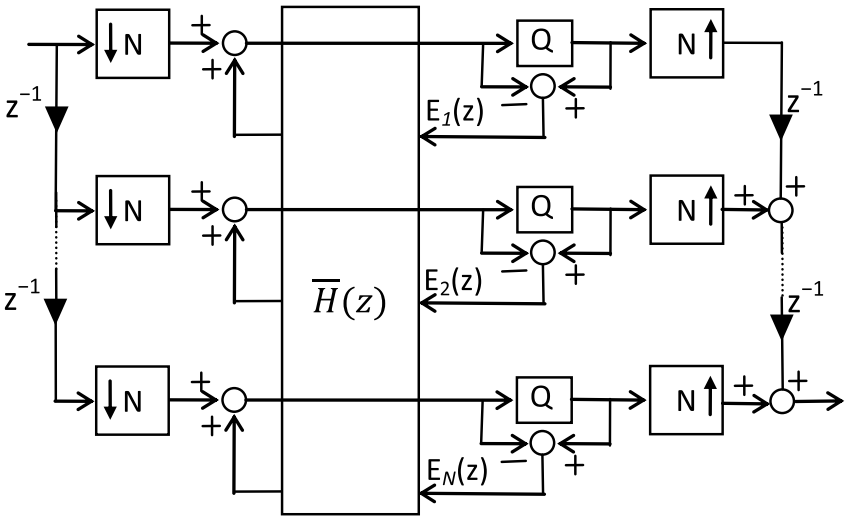

FIGURE 2 Time-interleaving architecture of the modulator in Figure 1. $E_i(z)$ is the error of the i-th quantiser

and q_k are the coefficients of the FIR filter $Q(z)$; that is, $Q(z) = \sum_k q_k z^{-k}$.

The reformulation can be done as follows [14]. Let

$$p_i = r_i \exp(j\alpha_i)(i = 0, 1, ..., L-1) \tag{8}$$

be the poles of the NTF, that is, the roots of $D(z)$, where r_i and α_i are the modulus and the phase of p_i, respectively. Then,

$$H(z) = \frac{\left[(1-z^{-1})^L - D(z)\right]}{\prod_{i=0}^{L-1}(1-p_i z^{-1})} \tag{9}$$

can be derived from (2). Every denominator term can now be transformed as

$$\frac{1}{(1-p_i z^{-1})} = \frac{(1-p_i^N z^{-N})}{(1-p_i z^{-1})(1-p_i^N z^{-N})} \tag{10}$$

where $p_i^N$is the N-th power of p_i. The term $(1-p_i^N z^{-N})$ can be factorised by means of their roots p_{ik} as

$$(1-p_i^N z^{-N}) = \prod_{k=0}^{N-1}(1-p_{ik} z^{-1}); p_{ik} = r_i \exp\left(j\alpha_i + \frac{j2\pi k}{N}\right) \tag{11}$$

Note that $p_{i0} = p_i$. Now, substituting Equation (11) in the numerator of (10), the terms $(1-p_i z^{-1})$ can be cancelled. As a result,

$$\frac{1}{(1-p_i z^{-1})} = \frac{\prod_{k=1}^{N-1}\left(1-p_{i,k} z^{-1}\right)}{(1-p_i^N z^{-N})} \tag{12}$$

Finally, substituting (12) in (9), Equation (5) can be obtained, being

$$Q(z) = \left[(1-z^{-1})^L - D(z)\right] \prod_{i=0}^{L-1} \prod_{k=1}^{N-1}\left(1-p_{i,k} z^{-1}\right)$$
$$P(z) = \prod_{i=0}^{L-1}(1-p_i^N z^{-1}) \tag{13}$$

The polynomials in (13) can be evaluated using numerical-computing programs like Matlab®. In practice, the NTF (Butterworth, Chebyshev...) is a rational function with real coefficients, so all poles are complex conjugates except for L odd, for which there is one additional real pole. As long as $H(z)$, obtained from (2) or (5), is also a rational function with real coefficients, in spite of the fact that the roots p_{ik} are complex numbers, the resulting coefficients of $Q(z)$ and $P(z)$ must be real numbers. Then, the imaginary terms are necessarily cancelled. In any case, if both polynomials are to be computed using real numbers, the expressions in (13) can be modified, as shown in Appendix I.

3 | COEFFICIENT ROUNDING

Let us now show an example of a third-order single-bit modulator ($L = 3$) for the case $N = 2$. The NTF chosen is a Butterworth high-pass transfer function with a normalised cutoff frequency (for a sampling rate $f_s = 2$ Hz) f_C. As the cutoff frequency increases, the quantisation noise is more abruptly attenuated at low frequencies, but on the other hand, it is amplified with greater gain at high frequencies. The high-frequency noise could overload the quantiser (making the modulator more prone to instability), and the maximum achievable amplitude of the input signal would decrease [5]. The dynamic range (i.e., the difference in decibels between the maximum input amplitude and the amplitude where the signal-to-noise-and-distortion ratio—SNDR—is 0 dB) has been obtained from simulations of the EF-SDM architecture for different values of f_C. The results are shown in Figure 3. The value $f_C = 0.16$ Hz represents a good trade-off between signal swing and modulator performance.

The transfer function poles are located in $p_0 = 0.5914$, and $p_{1,2} = 0.7062 \pm j\,0.3362$. From these floating-point quantities, the derived coefficients of polynomials in (13) will be also floating-point numbers, and therefore they must be codified with a large number of bits. As a consequence, digital implementation of the resulting architecture will be extremely complex or even unfeasible at high frequencies. Some kind of rounding is necessary to derive coefficients with only a few bits different to zero so the multipliers, which implement the product of a coefficient with its corresponding signal, can be replaced by a few adders.

TI architectures are very prone to mismatch in the gain between the N parallel paths, and also to deviations in the implemented transfer functions from their theoretical expressions [10]. In an analogue realisation, mismatch can be produced by tolerances in the components (resistors, capacitors…) or by non-linear effects in the amplifiers (finite DC gain, speed limitations…). In a digital implementation, these deviations come from coefficient rounding.

Figure 4 shows the NTFs for the floating-point (ideal) and rounded coefficients. The ideal NTF is evaluated from (1) for the poles given above. The rounded-coefficient NTF is calculated from the polynomials given in (13) whose coefficients are firstly calculated in floating-point format from the poles given above and secondly rounded to 11 bits[1] (the weights of the most and least significant bits being 1 and 2^{-10}, respectively). Finally, the NTF is calculated as $1 + H(z)$, where $H(z)$ is given by (5). As expected, the ideal NTF falls at low frequencies at a rate of −60 dB/dec. Unfortunately, rounding shifts the original zeros at $z = 1$ to the values $z_0 = 0.9403$, and

[1]This number has been arbitrarily chosen for the sole purpose of illustrating how rounding affects the NTF.

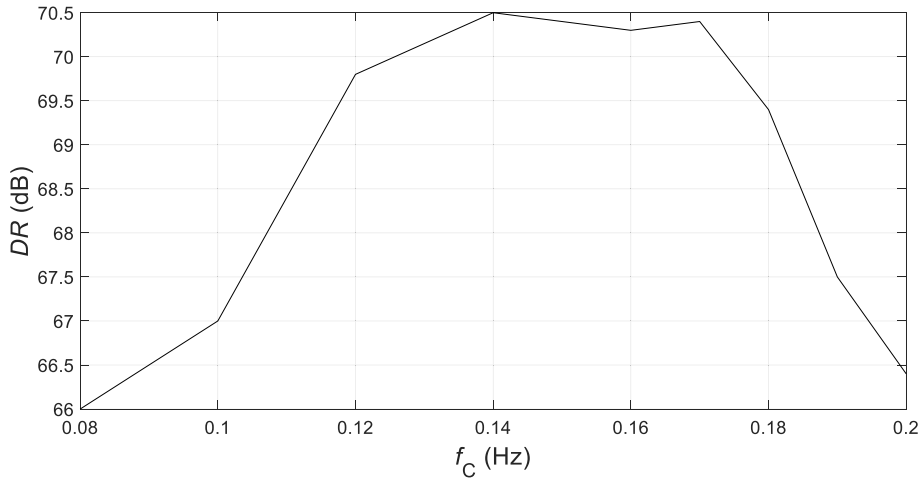

FIGURE 3 Dynamic range versus the cutoff frequency of the Butterworth third-order noise transfer function

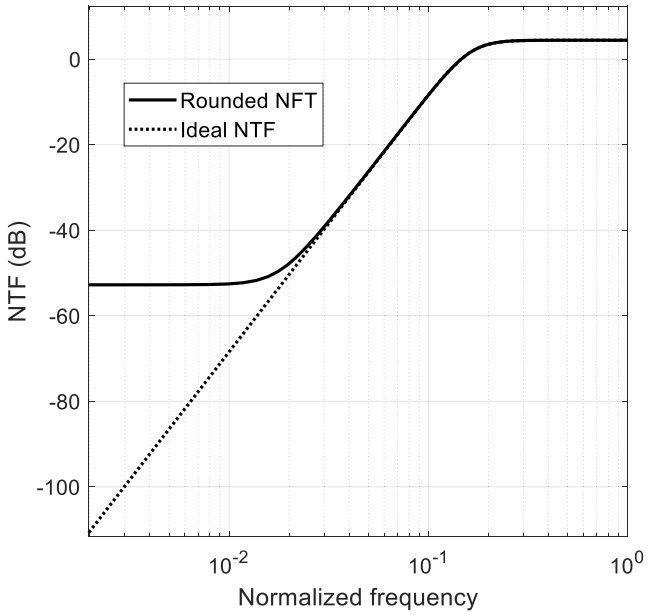

FIGURE 4 Third-order Butterworth noise transfer function (NTF) for floating-point (ideal) and 11-bit rounded coefficients

$z_{1,2} = 1.0297 \pm j\,0.0501$. In consequence, the NTF does not asymptotically fall to $-\infty$ dB and remains flat about $|1-z_0| \times |1-z_1|^2$ (approximately -50 dB) at low frequencies.

To guarantee that the original zeros will remain at $z = 1$ after rounding, we can proceed as follows. The poles of the original NTF given in (1) are rounded to the lowest possible resolution without compromising stability and performance. The new denominator of the NTF is recalculated from the rounded poles, $p_k^{(R)}$; that is,

$$D_R(z) = \prod_k \left(1 - p_k^{(R)} z^{-1}\right); k = 1, \ldots, L \tag{14}$$

Finally, the polynomials $Q(z)$ and $P(z)$ are calculated from (13) using the rounded poles and $D_R(z)$. In this way, $H(z)$ is calculated from (5) and the NTF, which is equal to $1 + H(z)$, is given by (1), as long as $D(z)$ is replaced by $D_R(z)$. As a consequence, the L zeros are maintained at $z = 1$.

4 | SIMULATION RESULTS

Following the procedure given above, simulations show that rounded poles with only 2-bit resolution are enough to guarantee the stability and performance of the resulting TI modulator. Then, the original poles ($p_0 = 0.5914$, and $p_{1,2} = 0.7062 \pm j\,0.3362$) are rounded to $p_0{}^{(R)} = 0.5$, and $p_{1,2}{}^{(R)} = 0.75 \pm \mathrm{j}\,0.25$. The polynomials in (13) can be calculated using $p_k^{(R)}$ and $D_R(z)$. The resulting coefficients are shown in the second column of Table 1. An additional 7-bit rounding can be done to them to obtain the third column of Table 1. Note that only the coefficients q_6 and p_3 are affected by this second rounding. Consequently, the maximum number of non-zero bits was limited to three, which simplifies the digital implementation of the filters.

Once $Q(z)$ and $P(z)$ are known, the PD of $H(z)$ can be obtained from (6)–(7), and the filter bank components can be represented as fractional functions; that is,

$$\overline{H}(z) = \left[H_{ij}(z)\right] = \left[\frac{N_{ij}(z)}{P(z)}\right] \tag{15}$$

where

$$\begin{aligned} N_{11}(z) &= q_2 z^{-1} + q_4 z^{-2} + q_6 z^{-3}; \quad N_{22}(z) = N_{11}(z) \\ N_{12}(z) &= q_1 + q_3 z^{-1} + q_5 z^{-2}; \quad N_{21}(z) = z^{-1} N_{12}(z) \end{aligned} \tag{16}$$

Figure 5 depicts the amplitude response of the floating-point, only pole rounding, and double-rounding implementations of the NTFs. The last two NTFs have been calculated using the coefficients given in the second and third columns, respectively, of Table 1. Once again, NTF is calculated as $1 +$

TABLE 1 Coefficients (in binary) of $Q(z)$ and $P(z)$

Filter coefficients			
		2-bit pole rounding	2-bit pole and 7-bit coefficient rounding
$Q(z)$	q_1	−1.00000000	−1.000000
	q_2	−0.01100000	−0.011000
	q_3	+1.00110000	+1.001100
	q_4	+0.10001100	+0.100011
	q_5	−0.01110000	−0.011100
	q_6	−0.00110111	−0.001110
$P(z)$	b_0	+1.00000000	+1.000000
	b_1	−1.01000000	−1.010000
	b_2	+0.10100100	+0.101001
	b_3	−0.00011001	−0.000110

Notes: Second column: coefficients obtained from rounded poles. Third column: Coefficients of the second column with additional rounding.

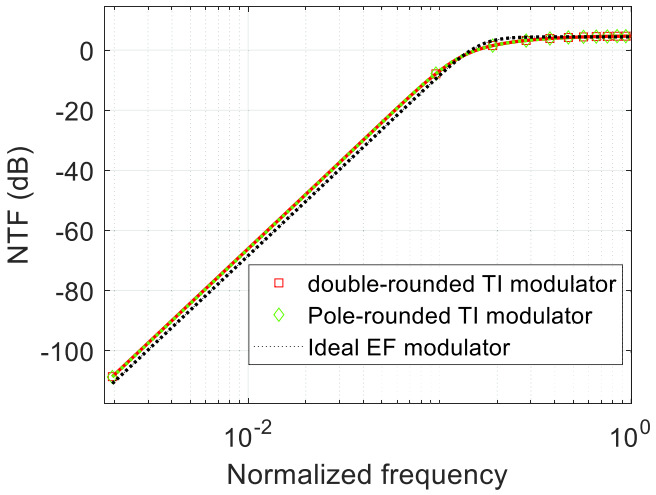

FIGURE 5 Third-order Butterworth noise transfer functions for the ideal, 2-bit rounded poles and additional rounded coefficients (2-bit pole and 7-bit coefficient rounding) cases

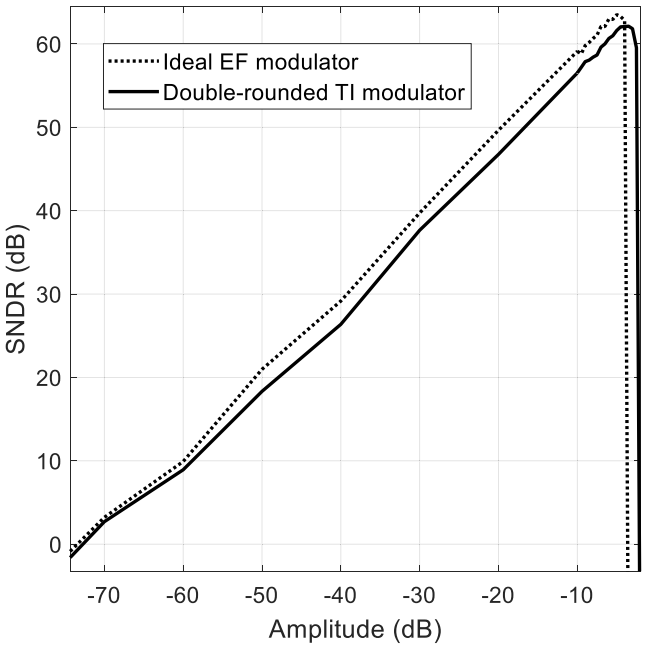

FIGURE 6 Signal-to-noise-and-distortion ratio (SNDR) curves for the error-feedback with ideal coefficient (Figure 1) and double-rounded time-interleaving (Figure 2) architectures

$H(z)$, where $H(z)$ is given by (5), their three zeros are placed at $z = 1$ (the additional rounding hardly affects performance in this case), and there is an attenuation loss of approximately 2 dB at low frequencies compared with the ideal NTF. As shown in Figure 5, the difference between both rounded NTFs is not appreciable

Time-domain simulations of the EF modulator (Figure 1) and its double-rounded TI (Figure 2) implementations, clocked at the rates f_s and $f_s/2$, respectively, are performed using MATLAB® & Simulink® for the third-order single-bit SDM with a cutoff normalised frequency of 0.16, which is the same used in the examples discussed previously. The original poles of the Butterworth NTF have been used for the EF modulator implementation, and the double-rounded coefficient (third column in Table 1) for that of the TI. The resulting SNDR curves are shown in Figure 6, where the noise power has been calculated in a bandwidth of $f_s/64$ ($OSR = 32$). Both curves match very well. The achieved DR values are 67.8 and 68.5 dB, which correspond to effective numbers of 11 and 11.12 bits for the EF and TI architectures, respectively. For sake of comparison, the second-order SDM has also been simulated with an OSR of 32 and $NTF = (1 - z^{-1})^2$. The third-order modulators outperform the second-order one by approximately 9 dB (1.5 effective bits). Finally, the power spectral densities of both third-order architectures are shown in Figure 7 for an input tone with −4 dB amplitude (full scale) and 0.0062 Hz frequency (approximately one-fifth of the signal bandwidth). The vertical dashed line marks the limit of the

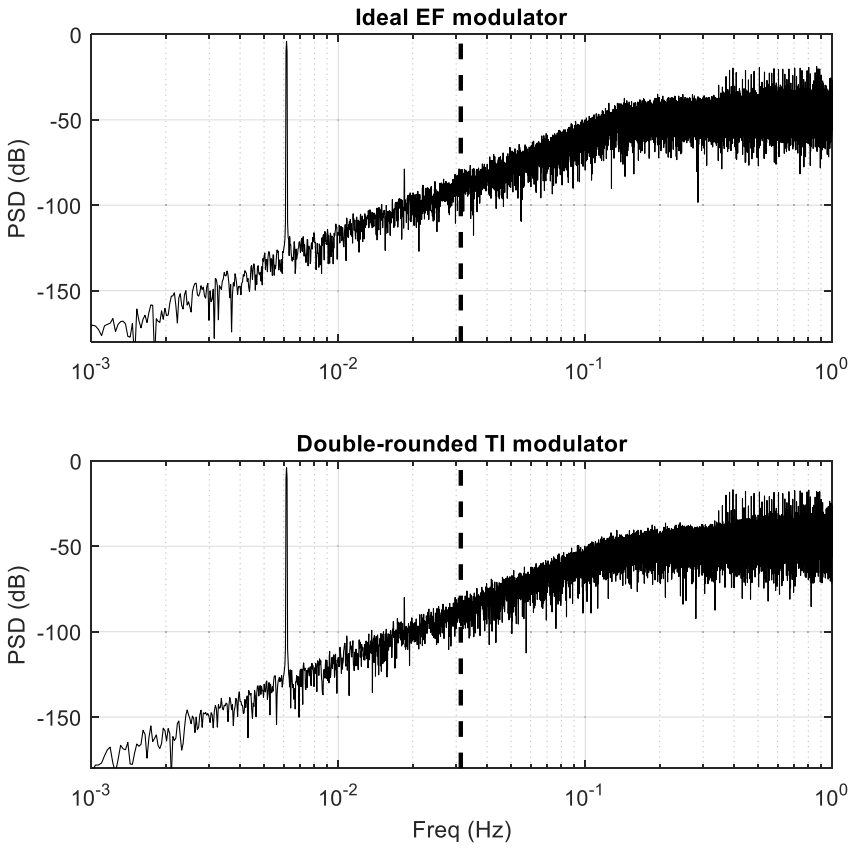

FIGURE 7 Power spectral densities of the ideal error-feedback (EF) and double-rounding time-interleaving (TI) modulators versus the normalised frequency (1 Hz corresponds to the clock rate of the TI modulator, f_s)

signal bandwidth (0.0313 Hz). The SNDR values are 62.41 and 61.65 dB, and the spurious free dynamic range values are 74.8 and 76.8 dB, for the ideal EF and the double-rounded TI modulators, respectively.

5 | CONCLUSIONS

The transformation of an EF SDM into its TI counterpart is not a straightforward task when the NTF is of the IIR type. This kind of modulator finds application as a DAC in the transmitters of increasingly demanding communication standards. A systematic procedure for this transformation is presented here for a single-bit modulator. To reduce the complexity of digital implementation of the TI SDM, the coefficients of the transfer functions are rounded to a low resolution (so that only a few bits are different to zero). A method to reach this objective is also proposed based on pole rounding. As a result, the rounded NTF retains its zeros at $z = 1$. The case study selected for this analysis (the two-phase decomposition of a third-order Butterworth high-pass NTF) shows that TI modulators with an IIR NTF can be implemented with low-resolution coefficients. The method proposed here can be also applied to EF modulators with the zeros of its NTF distributed in the signal band. In this case, the results obtained with the technique proposed for rounding coefficients could cause a loss in performance, which must be carefully monitored.

ACKNOWLEDGEMENT

This project has been funded by the Spanish Ministry of Science, Innovation and Universities in the project eMIDHE (RTI2018-099189-B-C21)

ORCID

Francisco Colodro https://orcid.org/0000-0001-6108-6117
Juana Maria Martinez-Heredia https://orcid.org/0000-0002-0459-6839
Jose L. Mora https://orcid.org/0000-0002-1186-8150
Antonio Torralba https://orcid.org/0000-0001-6887-6146

REFERENCES

1. Li, H., et al.: A 21-GS/s single-bit second-order delta-sigma modulator for FPGAs. IEEE Trans. Circuits Syst. 66, 482–486 (2019). https://doi.org/10.1109/TCSII.2018.2855962
2. Bhide, A., Alvandpour, A.: An 11 GS/s 1.1 GHz bandwidth interleaved ΔΣ DAC for 60 GHz radio in 65 nm CMOS. IEEE J. Solid-State Circuits. 50(10), 2306–2318 (2015). https://doi.org/10.1109/JSSC.2015.2460375
3. Tanio, M., et al.: An FPGA-based all-digital transmitter with 9.6 GHz 2nd order time-interleaved delta-sigma modulation for 500 MHz bandwidth. In: IEEE MTT-S International Microwave Symposium Digest, pp. 149–152.Honololu (2017)
4. Dinis, D.C., et al.: A fully parallel architecture for designing frequency-agile and real-time reconfigurable FPGA-based RF digital transmitters. IEEE Trans. Microwave Theory Tech. 66(3), 1489–1499 (2018). https://doi.org/10.1109/TMTT.2017.2764451
5. Norsworthy, S.R., Schreier, R., Temes, G.C.: Delta-Sigma Data Converters: Theory, Design and Simulation. IEEE Press, New York (1997)

6. Kiss, P., et al.: Stable high-order delta-sigma digital-to-analog converters. IEEE Trans. Circuits Syst. I. 51(1), 200–205 (2004). https://doi.org/10.1109/TCSI.2003.821283
7. Krukowski, A., Kale, I.I.: DSP System Design: Complexity Reduced IIR Filter Implementation for Practical Applications. Kluwer Academic Publishers, Dordrecht (2003)
8. Krukowski, A., et al.: Decomposition of IIR transfer functions into parallel, arbitrary-order IIR subfilters, Nordic Signal Processing Symposium. (NORSIG'96), Espoo, pp. 24–27 (1996)
9. Khoini-Poorfard, R., Johns, D.A.: Time-interleaved oversampling converters. Electron. Lett. 29(19), 1673–1674 (1993). https://doi.org/10.1049/el:19931112
10. Khoini-Poorfard, R., Lim, L.B., Johns, D.A.: Time-interleaved oversampling A/D converters: theory and practice. IEEE Trans. Circuits Syst. II. 44(8), 634–645 (1997). https://doi.org/10.1109/82.618037
11. Pham, J., Carusone, A.C.: A time-interleaved ΔΣ-DAC architecture clocked at the nyquist rate. IEEE Trans. Circuits Syst. II. 55(9), 858–862 (2008). https://doi.org/10.1109/TCSII.2008.923426
12. Podsiadlik, T., Farrell, R.: Time-Interleaved ΣΔ modulators for FPGAs. IEEE Trans. Circuits Syst. II. 61(10), 808–812 (2014). https://doi.org/10.1109/TCSII.2014.2345293
13. Vaidyanathan, P.P.: Multirate systems and filter banks. Prentice Hall, Englewood Cliffs (1993)
14. Bellanger, M., Bonnerot, G., Coudreuse, M.: Digital filtering by polyphase network: application to sample-rate alteration and filter banks. IEEE Trans. Acoust. Speech Signal Process. 24(2), 109–114 (1976). https://doi.org/10.1109/TASSP.1976.1162788
15. López-Valcarce, R., Mosquera, C., Pérez-González, F.: Hyperstable Adaptative IIR algorithms with polyphase structures: analysis and design. IEEE Trans. Signal Process. 47(7), 2043–2046 (1999). https://doi.org/10.1109/78.771052

How to cite this article: Colodro, F., et al.: Time-interleaving design of error-feedback sigma-delta modulators with infinite impulse response noise transfer function. IET Circuits Devices Syst. 15(5), 448–454 (2021). https://doi.org/10.1049/cds2.12040

APPENDIX I

Transformation of Equation (13)

If the pole p_i is real ($\alpha_i = 180°$), then it can be stated from the second equation of (11) that $p_{i\,k}$ and $p_{i\,N\text{-}k}$ are conjugates; they can be grouped, and (12) can be expressed as

$$\frac{1}{\left(1-p_i z^{-1}\right)} = \begin{cases} \dfrac{\prod_{k=1}^{(N-1)/2}\left(1-2\Re_e\{p_{ik}\}z^{-1}+|p_{ik}|^2 z^{-2}\right)}{1-p_i^N z^{-N}}; N \text{ odd} \\ \dfrac{\left(1+p_i z^{-1}\right)\prod_{k=1}^{(N-2)/2}\left(1-2\Re_e\{p_{ik}\}z^{-1}+|p_{ik}|^2 z^{-2}\right)}{1-p_i^N z^{-N}}; N \text{ even} \end{cases} \tag{17}$$

where as usual, $\Re$e(x) is the real component of x, and $|x|$, its modulus. On the other hand, if p_q and p_r are conjugates, every pole $p_{q\,k}$ is a conjugate of $p_{r\,N\text{-}k}$. Again, they can be grouped, and

$$\frac{1}{\left(1-p_q z^{-1}\right)\left(1-p_q^* z^{-1}\right)} = \frac{\prod_{k=1}^{N-1}\left(1-2\Re_e\left\{p_{qk}\right\}z^{-1}+\left|p_{qk}\right|^2 z^{-2}\right)}{1-2\Re_e\left\{p_q^N\right\}z^{-N}+\left|p_q\right|^{2N} z^{-2N}} \tag{18}$$

Summarising, for NTFs with real coefficients, the expressions in (17) and (18) can be substituted in (9), and $H(z)$ can be expressed in (5) as a rational function with real coefficients.